



ARTICLE



Varying weighted spatial quality assessment for high resolution satellite image pan-sharpening

Soroosh Mehravar^a, Farzaneh Dadress Javan^{id a,b}, Farhad Samadzadegan^{id a}, Ahmad Toosi^a, Armin Moghimi^c, Reza Khatami^d and Alfred Stein^b

^aDepartment of Geomatics, University College of Engineering, University of Tehran, Tehran, Iran;

^bDepartment of Geo-Information Science and Earth Observation (ITC), University of Twente, Enschede, The Netherlands; ^cDepartment of the Photogrammetry and Remote Sensing, Geomatics and Geodesy

Engineering Faculty, K.N.Toosi University of Technology, Tehran, Iran; ^dGeography Department, University of Florida, Gainesville, FL, United States

ABSTRACT

This paper focuses on spatial quality assessment of pan-sharpened imagery that contains valuable information of input images. Its aim is to show that fusion functions respond differently to different types of landscapes. It compares a quality assessment of an object-level procedure with that of a conventional pixel-level-based procedure which assigns uniform quality scores to all image pixels of pan-sharpened images. To do so, after performing a series of pan-sharpening evaluations, a weighted procedure for spatial quality assessments of pan-sharpening products, allocating spatially varying weight factors to the image pixels proportional to their level of spatial information content is proposed. All experiments are performed using five high-resolution image datasets using fusion products produced by three common pan-sharpening algorithms. The datasets are acquired from WorldView-2, QuickBird, and IKONOS. Experimental results show that the spatial distortion of fused images for the class vegetation cover exceeds that of man-made structures, reaching more than 4% in some cases. Our procedure can preclude illogical fidelity estimations occurring when pan-sharpened images contain different land covers. Since particular image structures are of high importance in remote sensing applications, our procedure provides a purpose-oriented estimation of the spatial quality for pan-sharpened images in comparison with conventional procedures.

ARTICLE HISTORY

Received 8 December 2020

Accepted 15 April 2021

KEYWORDS

Spatial quality; weighted average; object-level evaluation; pan-sharpened satellite imagery; impact of landscape

1. Introduction

Most high-spatial-resolution satellite imagery products provide both high-spatial-resolution panchromatic (PAN) images and Multispectral (MS) images containing rich spectral information but low spatial resolutions (Thomas and Wald 2004, Aiazzi *et al.* 2012, Snehmani *et al.* 2017). To take advantage of the information content in both images, pan-sharpening image fusion has been proposed to produce fused (pan-sharpened)

CONTACT Farzaneh Dadress Javan fdadrasjavan@ut.ac.ir Department of Geomatics, University College of Engineering, University of Tehran, Tehran, Iran; Department of Geo-Information Science and Earth Observation (ITC), University of Twente, 7522 NB Enschede, The Netherlands

© 2021 Informa UK Limited, trading as Taylor & Francis Group

images that contain both rich spectral and high spatial resolution information of input PAN and MS images (Choi *et al.* 2005, Alparone *et al.* 2007, Ehlers *et al.* 2010, Javan *et al.* 2021). Fusion methods developed so far have imperfections which means parts of spatial and spectral information of the input images could be lost during the fusion (Gilbertson *et al.* 2017, Xing *et al.* 2018). Furthermore, pan-sharpened images are widely used in a variety of applications, such as classification, landslide monitoring (Nichol and Wong 2005), tree species mapping (Castillejo-González 2018, Hlatshwayo *et al.* 2019), change detection (Bovolo *et al.* 2009, Moghimi *et al.* 2020), snow mapping (Sirguey *et al.* 2008) and extraction, identification, and reconstruction of image objects (Mohammadzadeh *et al.* 2006, Javan *et al.* 2013). The quality of the products that use pan-sharpened images is associated with the quality of fusion and thereby, many researches performed pan-sharpening quality estimations (Du *et al.* 2007, Alimuddin *et al.* 2012, Makarau *et al.* 2012, Jagalingam and Hegde 2015, Nikolakopoulos and Oikonomidis 2015, Wang *et al.* 2016, Duran *et al.* 2017, Li *et al.* 2017).

The main purpose of pan-sharpening methods is to produce fused images in a way that their spectral and spatial features match the initial MS and PAN images, respectively (Zhang 2008, Mitchell 2010). Due to the lack of perfect reference images to be used in image quality assessment (IQA), different protocols, such as Wald's protocol (Wald *et al.* 1997), Zhou's protocol (Zhou *et al.* 1998), Quality with No Reference (QNR) (Alparone *et al.* 2008), and Khan's protocol (Khan *et al.* 2009) have been proposed for quality assessment of pan-sharpening products (Palubinskas 2015). Commonly, the spatial quality of fusion products is estimated by comparing pan-sharpened images with the PAN data as the alternative reference images (Zhou *et al.* 1998, Karam *et al.* 2009, Al-Wassai and Kalyankar 2012).

1.1. Conventional strategies for quality assessment of pan-sharpened images

In the conventional pan-sharpening IQA methods, all image pixels take part in the IQA estimations as a whole set, leading to a unique quality score for the whole image. This procedure is known as pixel-level strategy (Samadzadegan and Javan 2013, Freire *et al.* 2014, Rodríguez-Esparragón *et al.* 2017). The quality measures reported by such procedures do not provide any information on spatial patterns of quality variations (Samadzadegan and DadrasJavan 2011). To address this issue, several researches in the literature have attempted to employ object-level IQA for pan-sharpening studies.

As an initial study, DadrasJavan and Samadzadegan (2014) have proposed an object-level strategy for the quality assessment of pan-sharpening products. Then, Dehnavi and Mohammadzadeh (2015) performed a class-based fusion to find out the best parameters of some fusion methods which are suitable for particular land covers. Hasanolou and Saradjian (2016) separated high-frequency regions from low-frequency parts in the pan-sharpened image to conduct the radiometric and geometric assessment in the corresponding separated image contents. Rodríguez-Esparragón *et al.* (2017) have followed an outline initiated by performing the watershed segmentation on their pan-sharpened images. Then they employed a spectral and an SQA metric to generate the spectral and spatial quality maps for their image objects. Liu, Huang and Li (2020) also followed the object-level IQA of pan-sharpened images. Using several quality indices, they evaluated and compared the performance of multiple pan-sharpening methods by different image

regions and land covers. Toosi *et al.* (2020) have also performed object-based spectral quality assessments on homogeneous objects, which had similar spectral and textural patterns.

By comparing the conventional assessment methods in this study, we have shown how the spatial quality of fused images produced by pan-sharpening algorithms is variant in different land covers of images.

1.2. Spatial quality assessment of pan-sharpened images

State-of-the-art SQA methods proposed in the field of computer vision and image processing aim towards becoming closer to the human visual system (HVS) and benchmarking it (Shi *et al.* 2018, Agudelo-Medina *et al.* 2019). From the HVS point of view, human eyes are more sensitive to the stronger edge strengths and detailed information of an image (Zhang *et al.* 2013, Wang *et al.* 2015, Wen *et al.* 2017). This scheme has led to the addition of a weighted pooling step to many of the SQA metrics (Ferzli and Karam 2009, Hong *et al.* 2016, Ni *et al.* 2016). These procedures take into account the locally estimated qualities with different weights that are proportionate to the spatial information level of their local regions.

Currently, no universally accepted IQA method is highly consistent with human abilities in detecting distortions of pan-sharpened images (Vivone *et al.* 2014). Few studies have attempted to develop and enhance the efficiency and robustness of IQA procedures suited for the pan-sharpening product's evaluation (Wang and Bovik 2002; Javan, Samadzadegan and Reinartz 2013, Alparone *et al.* 2018, Agudelo-Medina *et al.* 2019).

While edge strengths and detailed information vary per-pixel in a pan-sharpened image, the current SQA metrics consider the importance of all image pixels equally. Since the image quality is space-variant, it is better to yield a method for pooling the local qualities instead of an overall score attained by averaging. Moreover, the spatial consistency of sharp details is of more importance in many Remote Sensing (RS) applications (Freire *et al.* 2014, Alparone *et al.* 2018).

Many researches in the field of image quality, tried to propose quality assessment procedures that are correlated well with the perceptive mechanism of the human visual system. In this regard, because the human visual system is more sensitive to the stronger edge strengths and detailed information of an image (Zhang *et al.* 2013, Wang *et al.* 2015, Wen *et al.* 2017), such studies allocated varying weights (proportional to local spatial information content) to the locally estimated qualities (Wang and Shang 2006, Wang and Li 2010). Therefore, these quality assessment methods first estimate the local qualities, then employ a spatial pooling algorithm that combines the local qualities into a single quality score (Xue *et al.* 2013).

Spectral distortion in a fused image is also of considerable importance and even can cause spatial artefacts. Spectral distortions in pan-sharpened imagery can be produced by many factors, that is, haze effect (Jing and Cheng 2009, Meng *et al.* 2018) and misalignment of MS and PAN images (Jing and Cheng 2011a, Javan *et al.* 2019). Some studies have proposed successful fusion methods to take into account the impact of haze (Jing and Cheng 2011b, Li and Jing 2017) and misalignment of MS and PAN images (Li *et al.* 2018). Downscaling in a fusion process has essentially been an ill-posed, inverse problem, and there is inevitable information loss in downscaling solutions (Wang *et al.* 2019). Thus,

some studies have worked on useful methods that account for the PSF of the sensor to reduce the spectral/spatial information loss caused by downscaling technique (Pardo-Igúzquiza, Chica-Olmo and Atkinson 2006, Pardo-Igúzquiza and Atkinson 2007, Pardo-Igúzquiza, Atkinson and Chica-Olmo 2010). Although the spectral and spatial contents of images are not completely separable, the spectral and spatial qualities are usually studied distinctly.

In the proposed SQA section of this study, we aimed to address this issue by proposing an efficient SQA procedure that can help the RS community with the purpose-oriented estimation of the spatial quality for pan-sharpened images. Using the proposed spatial quality assessment method along with accurate spectral quality assessment methods, the superior methods used for enhancing (pan-sharpening) the images can be reliably determined. After any image enhancement process and before the mapping projects (i.e. urban mapping, tree species mapping), the enhanced images should be spatially and spectrally assessed. The proposed method helps in finding the best image enhancement methods (i.e. pan-sharpening methods) that are suitable for mapping purposes.

For many RS applications, the quality of analysis is directly related to the spatial features of the images (Freire *et al.* 2014). Moreover, with the availability of very high-spatial-resolution satellite images, large-scale mapping of urban areas has become more popular recently (DadrasJavan *et al.* 2018). Thus, the Spatial Quality Assessment (SQA) of fusion products is the main focus of this research.

2. Materials and methods

To describe the problem involved in the conventional SQA methods, the issue is first described in the problem description (2.2) section. Therefore, we examined how fusion methods and the quality they provide are affected by different image contents. Since sharper structures are of more importance in many RS applications of satellite images, different weights should be allocated to each local SQA estimation. This point has led us to propose a spatially varying weighted strategy for SQA purposes in the proposed SQA (2.3.2) section. The SQA metrics used in this study are introduced in the following.

2.1. Spatial quality assessment metrics

In this research, the following SQA metrics are selected to be used. A brief description of each these metrics is presented in the following:

Gradient Magnitude Similarity (GMS): Considering the achieved gradient magnitudes of PAN and fused images named m_{PAN} and m_{Fused} , calculation of gradient magnitude similarity will be possible by Equation (1) where the variable i denotes the location (pixel number) in the image and c is a positive constant that supplies numerical stability (Xue *et al.* 2013, Wen *et al.* 2017).

$$GMS(i) = \frac{2m_{\text{pan}}(i)m_{\text{Fused}}(i) + c}{m_{\text{pan}}^2(i) + m_{\text{Fused}}^2(i) + c} \quad (1)$$

D_s : The spatial component of the QNR index is computed through similarity measurements of couples of scalar images executed by employing the universal image quality index (UIQI). Equation (2) represents the D_s component of the QNR metric, where MS_K is

the low-resolution Kth MS band, and PAN_L is the PAN image degraded to the resolution of MS image. Fused_K is the Kth band of pan-sharpened image and is defined to be compared with the original PAN image, and N denotes the number of MS bands. Also, q represents a constant value (Alparone *et al.* 2008, Palubinskas 2015).

$$D_S = \sqrt[q]{\frac{1}{N} \sum_{K=1}^N |\text{UIQI}(MS_K, \text{PAN}_L) - \text{UIQI}(\text{Fused}_K, \text{PAN})|^q} \quad (2)$$

Spatial Correlation Coefficient (SCC): This is the metric in which the high-frequency details of PAN and fused images are first extracted by a high-pass 2-D filter; then, correlation calculation is used for similarity determination of these detail maps (Klonus and Ehlers 2009, Pushparaj and Hegde 2017).

Edge Correlation Coefficient (Edge CC): In the case of Edge CC, the similarity value will be computed on the edge maps of PAN and fused images using the correlation definition (Ehlers *et al.* 2010).

Edge Preservation Ratio (EPR): The general EPR method consists of accuracy and robustness components, the former refers to the ratio of properly preserved edge pixels in the distorted image to the number of edge pixels in the reference image, and the latter indicates the ratio between the number of preserved edge pixels to the number of edge pixels in the distorted image (Yu *et al.* 2014).

Edge Variance Distortion (EVD): The EVD metric takes into account the edge differences and compares the edge map of the pan-sharpened image with the edge map of the PAN image to count the number of eliminated and extra edge pixels in the fused image (Qi *et al.* 2014).

2.2. Problem description

The limitations and challenges involved in the pixel-level and object-level SQA strategies used for the evaluation of pan-sharpened images can cause illogical quality estimations. In this section, it becomes clear how the spatial fidelity of fusion results is related to the type of landscape and the problems of the conventional strategies are clarified. The problem is that fusion quality is space-variant and conventional assessment methods do not take it into account. Although object-level IQA can provide more rigorous estimation than the pixel-level IQA, it still faces a challenge. The issue is that all image pixels inside an object are assumed to have identical quality.

We used several quality maps/charts to elaborate on the reason for deviations in conventional quality estimations. These maps/charts reveal that the spatial quality of fusion is not consistent in the pan-sharpened images. Using the object-level strategy, we showed that the quality of fusion products is space-variant. We then compared the pixel-level and object-level assessment results and discussed the problem. The general aim of object-level IQA is to calculate the quality within specific image objects. Contrary to the similar studies that set the image segments as their image objects for their object-level IQA calculations (i.e. DadrasJavan and Samadzadegan 2014, Restaino *et al.* 2016, Rodríguez-Esparragón *et al.* 2017), we arranged the image classes (derived from classification) as the objects for the object-level SQA to understand semantic relations between

specific land covers and fusion functions. In the following, the procedure of image object extraction and object-level SQA is explained.

2.2.1. Image object extraction

The objects used for object-level analyses are image classes in this paper. In this regard, segments of the MS image obtained by the multiresolution segmentation algorithm (MSA) are used to introduce training data to the supervised classification method. The MSA can minimise the average heterogeneity of image objects for the arbitrary scale parameter which determines the resolution of image objects (Trimble Documentation, 2014). MSA is known as a bottom-up region-merging technique which uses scale, colour and shape properties to define the homogeneity criterion (Darwish *et al.* 2003, Benz *et al.* 2004). The K-Nearest Neighbours (K-NN) classification method, which is a popular technique in RS applications (Chirici *et al.* 2016, Thanh Noi and Kappas 2018), has been used in this paper. Some created segments of the MS image have been used to set the check data for the validation process of classification.

2.2.2. Object-level versus pixel-level spatial quality assessment

The comparison between the extracted information in the corresponding land covers of the PAN and the fused image is considered as object-level SQA in this paper. The flowchart of our object-level SQA architecture is explicated in [Figure 1](#). In this paper, we conducted the object-level assessment within image classes obtained from the classification of up-sampled MS images. In this regard, after extracting the spatial information of fused and PAN images, the spatial information within the corresponding classes was extracted to be used for SQA. Consequently, the object-level assessment was performed separately for the spatial information found in each land cover (class boundary). In this procedure, the values of all corresponding pixels belonging to a specific land cover are compared with each other using SQA metrics.

On the other hand, pixel-level SQA is the most common strategy in which the whole set of image pixels are entered into quality computations. This strategy does not need any local quality estimation and only the extracted information of PAN and fused image are compared with each other directly.

2.3. Spatially varying weighted assessment

As noted before, the spatial features of image structures, such as buildings, roads, and some other man-made structures are commonly more important than that of flat areas (Freire *et al.* 2014). Besides, the HVS is more sensitive to sharp and detailed areas of an image.

To address the challenges of pixel-level and object-level strategies, we proposed a spatially varying weighted SQA procedure for pan-sharpened images. Apart from the proposed weighted procedure for SQA in [subsection 2.3.2](#), we examined four spatial features in [subsection 2.3.1](#) to find the suitable weight component for the proposed procedure. Weight component selection is not a part of the proposed SQA procedure and is only pursued to select the most suitable spatial feature that can be used as the weight component in the proposed method.

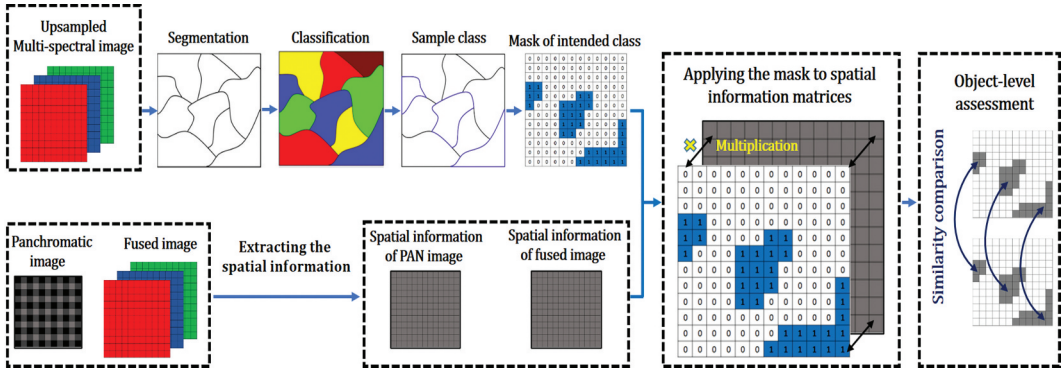


Figure 1. Diagram of the proposed scheme for object-level quality assessment.

2.3.1. Weight component selection

We have examined four spatial image features to select one of them as the weight factor. We assumed that the most suitable weight component can allocate larger weight factors to the detailed structures of images, that is, buildings and road class. To test the performance of such spatial features, we investigated which of these spatial features can assign larger weights to areas with higher spatial context (i.e. buildings and roads). Most SQA metrics in the field of image quality have employed a single spatial feature as the weight component, for example, saliency or gradient magnitude. However, few studies have examined the capability of different spatial features to find their weight component. In this paper, we compared four spatial features to select the best of which as the weight component for the proposed SQA procedure. To this end, as depicted in Figure 2, after extracting the spatial features from the PAN image, a normalisation of feature values was done to obtain comparable properties. Afterwards, the mean values of these attributes were computed in each class of the image. Since the details of a remotely sensed image are commonly dense and sharp in buildings and roads, one spatial feature (among the four techniques) that could assign relatively higher mean values to such land covers was recognised as the proper attribute for the weight component of our proposed procedure. Weight component selection does not belong to the proposed method and land covers are only used to evaluate the suitability of the spatial features for weighting the SQA procedure. We only used land covers to determine which spatial feature could better expose the spatial information of detailed areas. The determined spatial feature is supposed to be used for weighting the assessment in the proposed SQA.

The following four spatial feature extraction techniques were selected to accomplish the diagram of Figure 2. We used saliency feature that can denote the most important parts of an image from the HVS point of view (Hou and Zhang 2007). Saliency feature has been used as the weight component in many studies in the field of image quality, i.e. (Wen *et al.* 2017, Shi *et al.* 2018). Among multiple methods proposed for saliency extraction, i.e. (Hou and Zhang 2007; Guo, Ma and Zhang 2008, Qin *et al.* 2015), we used the algorithm proposed by Seo and Milanfar (2009) because of its popularity. We also used the high-pass spatial details of the PAN image extracted by the Laplacian filter (Zhou *et al.*

1998). Moreover, using the Gaussian filter we could extract the details by subtracting the low-pass version of PAN image from the original high-resolution PAN image. Gradient magnitude of Sobel operator, which has extensive applications in the field of image quality, is also selected to be compared with other attributes.

2.3.2. Proposed spatial quality assessment procedure

In this part, the procedure we used for weighting the SQA is defined. We aimed at using a weighted average assessment in a way that each of the locally calculated quality estimations participates in the overall quality estimation with a spatially varying weight factor. In this paper, we propose to improve four well-known SQA metrics, namely SCC, QNR-Ds, GMS and Edge CC by incorporating a spatially varying weight component into their equations. The novel idea can be generalised to all similar metrics as well.

As for Figure 3, the diagram is divided into three steps. In the first step, a pair of spatial detail maps (high spatial frequency information), related to the intended metrics, were extracted from the PAN and fused images. We called these maps 'objective matrices'. The second step describes some needed information about the application of the sliding window in the proposed SQA strategy. Based on our proposed scheme, the spatial metrics were calculated between the two groups of pixel values located inside the sliding windows of edited objective matrices. The local assessments are done within each movement of the sliding windows. Starting from the top-left corner, the sliding windows move through all rows and columns to reach the bottom-right corner of the image. The sliding window size is an arbitrary parameter that has to be an odd-dimensional square to define the central pixel of the window. This size parameter is selected equal to 3 in this paper. The central pixel of the sliding window in each movement takes a value from the corresponding pixel in the spatial feature matrix ($F_{(i,j)}$) which defines the weight factor. The sliding window shown by $W_{(i,j)}$ defines a 3×3 square block for a central pixel with (i,j) coordinate. The third step defines the way of adding weight factors to the conventional metrics using a weighted average formula. In each movement of the sliding window having a central pixel with (i,j) coordinate, an SQA metric is computed ($M_{W_{(i,j)}}$). In each movement of the sliding window, $M_{W_{(i,j)}}$ takes a unique weight ($F_{(i,j)}$). The denominator of the weighted average formula is the sum of the values of all pixels in the spatial feature matrix.

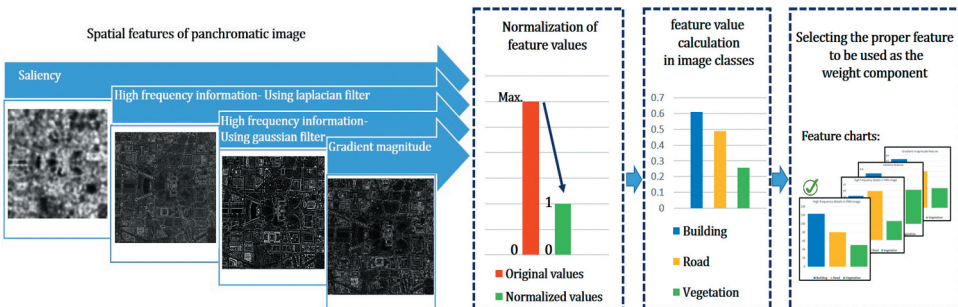


Figure 2. Determination of the most appropriate spatial feature to be used as the weight component.

Regarding the proposed strategy, the enhanced version of the mentioned original metrics is defined in the Equations (3)- (6) of [Table 1](#).

Similar to many state-of-the-art IQA methods like (Ferzli and Karam 2009, Hong *et al.* 2016, Ni *et al.* 2016), the proposed framework can be used to assign larger weights to the local qualities of areas with high spatial information context, hence becoming closer to the HVS mechanism in image quality assessment.

3. Experimental results

Five series of high-resolution satellite images as the input data sets including five pairs of PAN and MS images have been used ([Figure 4](#)) in this paper. Two of the data sets are taken from two distinct parts of a great image taken from Washington, DC. The data named Washington-1 are a part of an urban area with little vegetation cover, while Washington-2 data consists of a high amount of vegetation areas with less urban structures. A nearly equal portion of each land cover is seen in the third image set named Melbourne. The fourth data named India Chilika Lake contains a large extent of agricultural lands. The Sichuan data are also comprised of a large amount of vegetation and shadow. The descriptions of these data are presented in [Table 2](#).

Classes of the input MS images are extracted and shown in [Figure 4](#). The training and test areas for classification were selected from the segments created by MSA algorithm. The classification is conducted by K-NN classifier. Bare soil areas were merged with road class because of their spectral similarities. The validation of the performed classifications was done by comparing the classes with predefined test areas. The confusion matrix has been calculated and the attained results for the overall accuracy and kappa coefficient of the classified images are presented in [Table 3](#).

3.1. Results of pixel-level and object-level spatial quality assessment

The object-level quality assessment is performed based on the reviewed SQA metrics, namely EPR, GMS, QNR-Ds, Edge CC and EVD. Three well-known pan-sharpening methods, namely Matting Model Pan-sharpening (MMP) (Kang, Li and Benediktsson 2013), Modulation Transfer Function-Generalised Laplacian Pyramid (MTF-GLP) (Aiazz *et al.* 2002, 2006), and Weighted Wavelet Intensity (WWI) (Zhang and Hong 2005) are selected due to their successful performance reported by Javan *et al.* (2021).

To visually show the fact that the spatial quality of the pan-sharpened images varies from place to place, the EPR colour maps and the GMS quality maps are illustrated in [Figures 5](#) and [Figures 6](#), respectively. These maps are only generated for the WWI fusion method because the other methods have shown a highly similar pattern. We used the WWI fusion method because it is known as one of the most robust and efficient pan-sharpening algorithms in the literature (Javan *et al.* 2021). Pan-sharpened images produced by WWI usually show good spectral and spatial quality. However, no fusion method can inject all of the spatial information from PAN into the fused images. A significant trade-off between the spectral and spatial performance of the pan-sharpening algorithms has long been reported in the

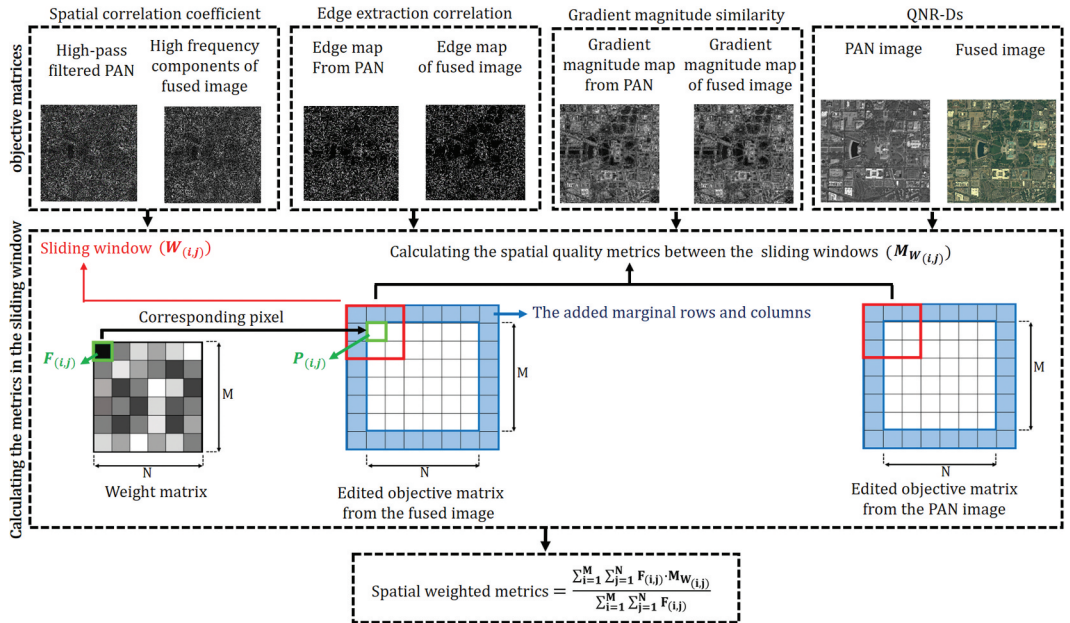


Figure 3. Proposed framework for varying weighted spatial quality assessment.

literature (Vivone *et al.* 2014). This means that the pan-sharpening algorithms having good spectral performance cannot efficiently preserve the spatial details and vice versa. The pixel-level quality maps of Figures 5 and Figures 6 can lay the ground to conceive that the fusion quality is space-variant. The EPR colour maps of Figure 5 consist of green, red, and white colours. The detected edge pixels of the PAN image, which were not recognised as edge pixels in the fused image, are shown in green colour. Contrarily, the pixels of fused images that are detected as edges but their corresponding pixel in the PAN image is not recognised as edge pixels are shown in red. Finally, those corresponding pixels of PAN and fused images that both were detected as edge pixels are specified by white, and black colour pixels are those which were not recognised as edges in any of the images.

In the GMS quality maps of Figure 6, the darker areas illustrate the lower similarities and the brighter pixels are those with higher GMS value. The obtained similarity maps clearly show that more spatial degradations occurred in vegetation covers (darker areas) while higher spatial quality preservations (better spatial quality shown by brighter pixels) can be seen in detailed structures of the images (i.e. buildings and roads) after the fusion.

In Figure 7, the object-level quality maps of the studied data sets are shown. These maps are derived from the results of QNR-Ds, Edge CC, EVD and SCC metrics in each land cover. We used different colours to denote different fusion qualities in different land cover objects. For example, the Washington-1 data has three classes, so the colour maps of this data contain three different colours indicating the fusion quality of the regions in each land cover object. Using the colour maps in Figure 7, we showed that the fusion quality varies between different land cover objects. For

Table 1. Improved spatial metrics by incorporating the weight component.

Names of weighted metrics	Equations of the weighted metrics	Descriptions
Weighted GMS (WGMS)	$WGMS = \frac{\sum_{i=1}^M \sum_{j=1}^N F_{(i,j)} \cdot GMS_{W_{(i,j)}}}{\sum_{i=1}^M \sum_{j=1}^N F_{(i,j)}} \quad (3)$	$GMS_{W_{(i,j)}}$, $SCC_{W_{(i,j)}}$, $EdgeCC_{W_{(i,j)}}$ and $Q_{W_{(i,j)}}$ are the original indices calculated within the window $W_{(i,j)}$
Weighted SCC (WSCC)	$WSCC = \frac{\sum_{i=1}^M \sum_{j=1}^N F_{(i,j)} \cdot SCC_{W_{(i,j)}}}{\sum_{i=1}^M \sum_{j=1}^N F_{(i,j)}} \quad (4)$	
Weighted Edge CC (WEdgeCC)	$WEdgeCC = \frac{\sum_{i=1}^M \sum_{j=1}^N F_{(i,j)} \cdot EdgeCC_{W_{(i,j)}}}{\sum_{i=1}^M \sum_{j=1}^N F_{(i,j)}} \quad (5)$	
Weighted QNR-Ds index (WQ)	$WQ = \frac{\sum_{i=1}^M \sum_{j=1}^N F_{(i,j)} \cdot Q_{W_{(i,j)}}}{\sum_{i=1}^M \sum_{j=1}^N F_{(i,j)}} \quad (6)$	

Table 2. Specification of applied data sets.

Name of data set	Sensor	Location	GSD at Nadir PAN-MS	Dimension of PAN image	Number of spectral bands
Washington-1	WorldView-2	Washington DC, USA	0.46 m-1.84 m	3584 × 3584 pixels	8 bands (red, blue, green, near-IR1, red edge, coastal, yellow, near-IR2)
Washington-2		Washington DC, USA		2496 × 2496 pixels	
Melbourne		Melbourne, Australia		1996 × 1996 pixels	
India Chilika lake	QuickBird	India, Odisha state	0.65 m-2.62 m	1024 × 1024	4 bands (Blue, Green, Red, Near IR)
Sichuan	IKONOS	China, Sichuan province	0.82 m-3.28 m	2048 × 2048	4 bands (Blue, Green, Red, Near IR)

Table 3. The classification input parameters, and the scores of overall accuracy and kappa coefficient for classified images.

Case study	No. of training samples	No. of test samples	Overall accuracy	Kappa coefficient
Washington-1	52	46	93.47%	90.83%
Washington-2	29	25	95.33%	93.02%
Melbourne	40	38	96.82%	95.31%
India Chilika lake	35	30	91.26%	89.88%
Sichuan	55	30	92.61%	90.47%

Table 4. The parameters of local self-resemblance used in Saliency detection.

Parameter Description	Value	Parameter Description	Value
Local adaptive regression kernel/window (LARK) size	3	Size of a centre surrounding region for computing self-resemblance	3
LARK sensitivity parameter	0.42		
LARK smoothing parameter	0.2	Fall-off parameter for self-resemblance	0.07

example, the fusion quality in vegetated areas differs from the fusion quality in buildings and roads.

In Figure 8, the quantitative quality results of the utilised pan-sharpening methods in every land cover are presented for our five data sets. According to the colour maps of Figure 7, a great discrepancy could be seen among the fusion quality scores of image classes as it attains even more than 10% in some cases. This shows that the pixel-level SQA strategy which assigns a single quality score to the fused image is not accurate. On the

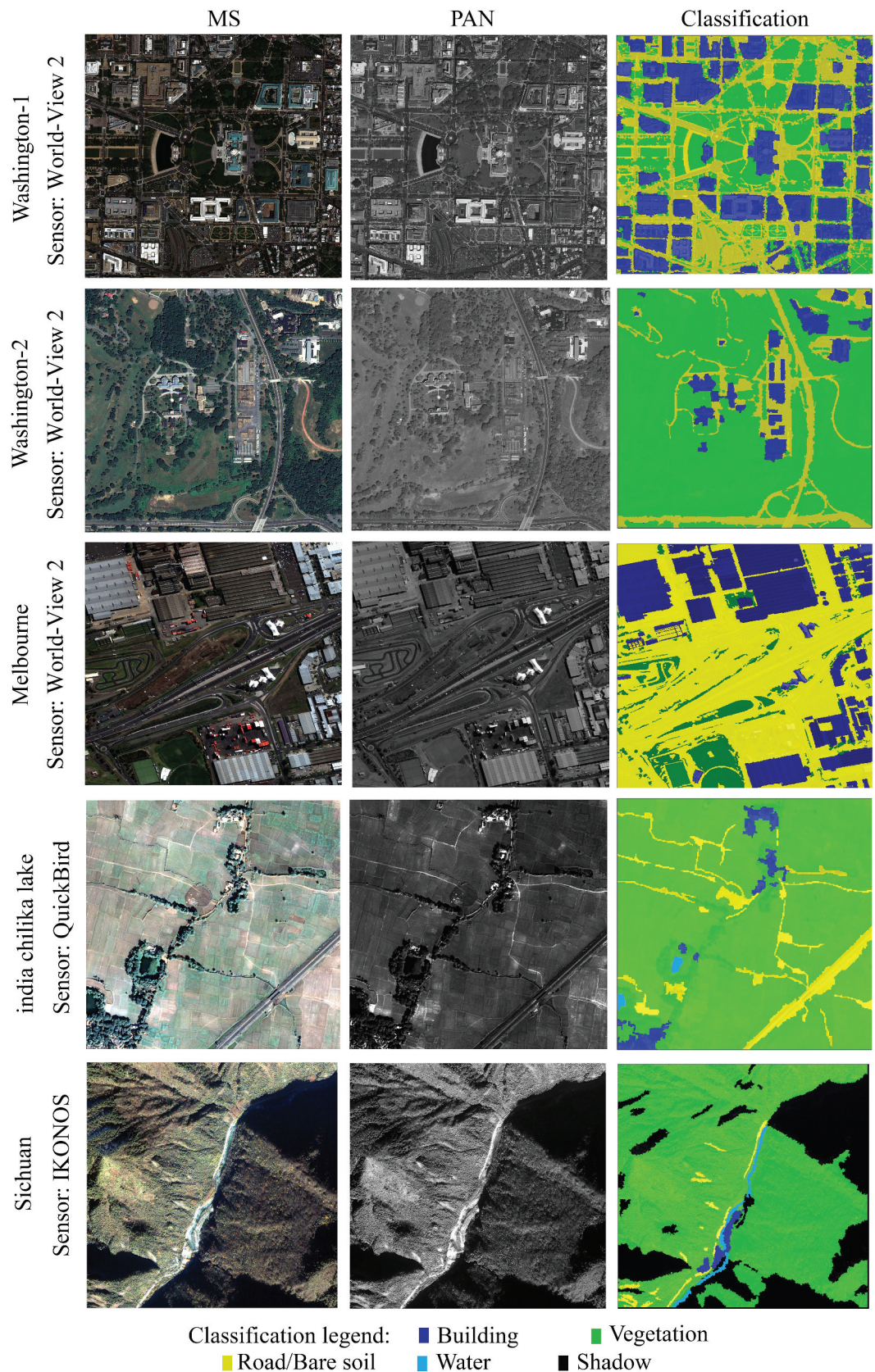


Figure 4. Five image sets and their corresponding classification maps.

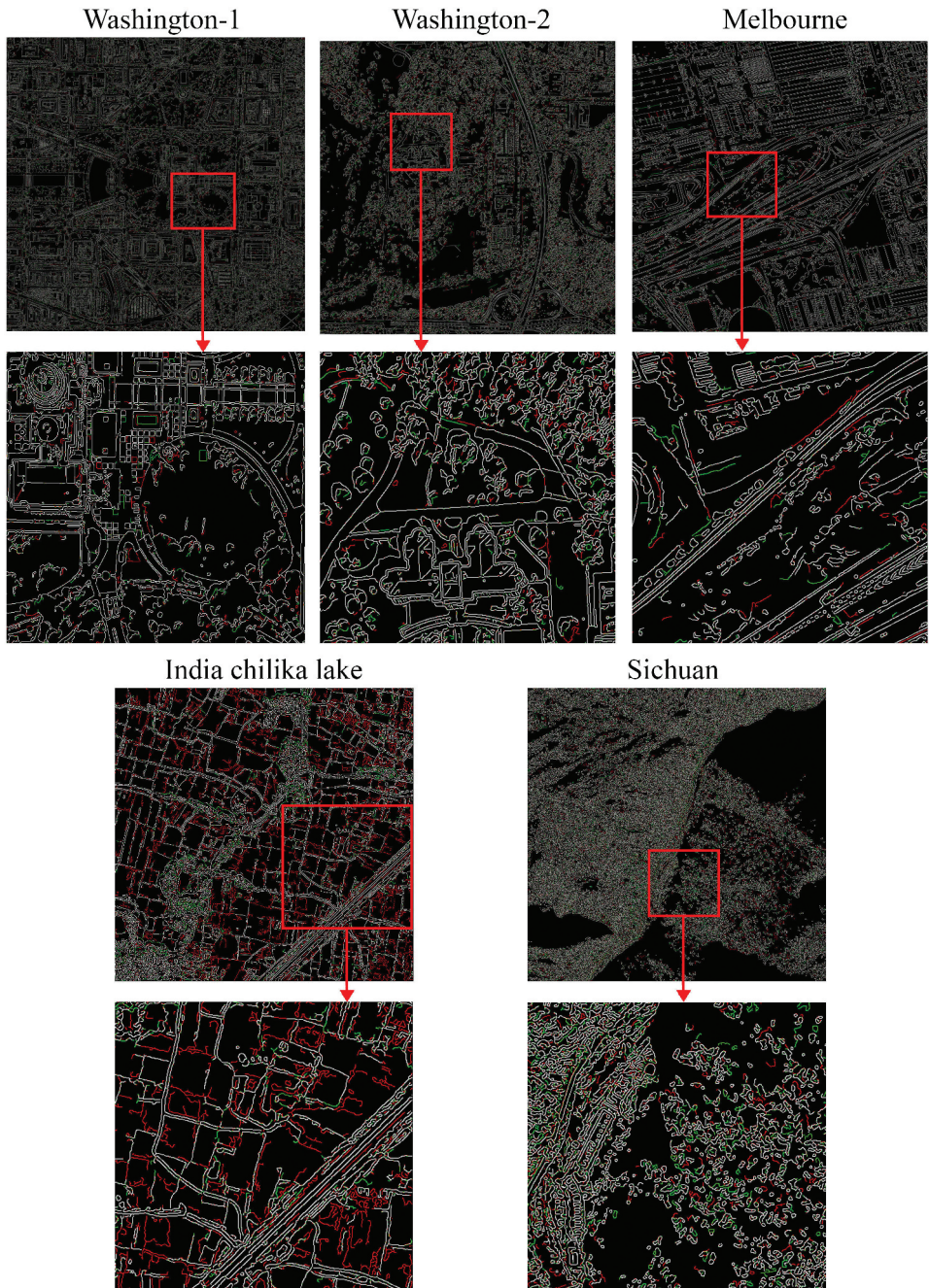


Figure 5. EPR quality maps of pan-sharpened images.

other hand, even assigning a single quality score to each class (object-level SQA) cannot accurately represent the fusion quality. This is because Figures 5 and Figures 6 indicated that fusion quality is variant even within a class.

Table 5. The results of the proposed and conventional assessment methods. C: Conventional method; P: Proposed method.

Metric	SCC [%]			Edge CC [%]			GMS [%]			QNR-Ds [%]		
	WWI	MMP	MTF-GLP	WWI	MMP	MTF-GLP	WWI	MMP	MTF-GLP	WWI	MMP	MTF-GLP
Fusion method												
Washington-1	C98.21	C97.53	C97.67	C77.64	C60.02	C63.37	C65.95	C53.24	C56.86	C0.77	C0.78	C0.47
	P98.01	P98.09	P97.86	P79.88	P61.45	P64.03	P67.33	P57.39	P59.06	P0.76	P0.75	P0.45
Melbourne	C98.22	C97.41	C97.79	C85.88	C68.44	C71.87	C65.51	C52.69	C55.75	C0.76	C0.81	C0.52
	P98.73	P97.7	P97.92	P87.14	P70.54	P72.77	P67.62	P55.73	P57.61	P0.73	P0.79	P0.49
Washington-2	C96.18	C95.12	C95.47	C70.08	C27.69	C55.02	C63.96	C50.92	C54.07	C0.83	C0.85	C0.28
	P98.68	P96.74	P96.98	P76.02	P42.83	P57.9	P68.05	P56.19	P58.32	P0.76	P0.76	P0.24
India Chilika lake	C97.19	C96.22	C96.48	C73.27	C67.14	C71.03	C56.36	C44.91	C47.22	C0.7	C0.82	C0.55
	P98.65	P97.83	P97.94	P77.13	P70.36	P73.08	P59.92	P48.54	P51.11	P0.63	P0.79	P0.51
Sichuan	C94.81	C94.16	C94.49	C77.56	C73.11	C75.03	C67.63	C56.07	C58.95	C0.72	C0.91	C0.7
	P96.58	P95.97	P96.33	P80.86	P75.4	P77.53	P69.41	P58.64	P60.77	P0.69	P0.88	P0.68

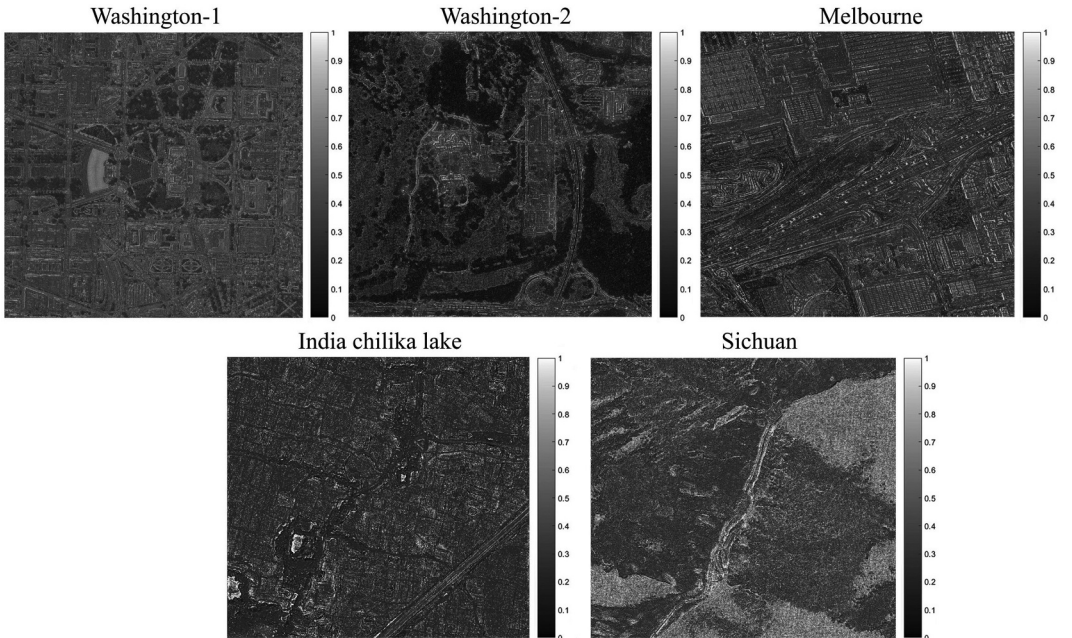


Figure 6. Gradient magnitude similarity maps from pan-sharpened images.

3.2. Proposed spatial quality assessment

3.2.1. Analysis of spatial features for weight component selection

As discussed before, saliency, Laplacian filter, Gaussian filter and gradient magnitude are used to determine the most appropriate spatial feature for weighting our proposed SQA strategy (Figure 9). The parameters related to the used saliency feature are presented in Table 4. We also used a rotationally symmetric low-pass Gaussian filter with a size of 64 and a standard deviation equal to 16 to obtain the other detail map. In the case of Laplacian filter and similar to İlkk et al. (2011), a conventional 3×3 size discrete approximation to the Laplacian filter is applied to the images using the convolution method. All parameters are also determined and selected by trial and error.

The mean values of extracted spatial features inside the image classes are computed and presented for all data sets in Figure 10. As was discussed previously, the feature which assigns higher mean values to spatially important objects (such as buildings and roads), is supposed to be selected as the weight factor in the proposed SQA procedure.

In the case of gradient magnitude in Figure 10, the discriminations between the intended classes denote the superiority of this feature among others. Consequently, we set the gradient magnitude as the weight factor for the proposed weighting procedure.

3.2.2. Difference between the proposed and conventional procedure

To visually conceive how high gradient magnitudes can represent the spatially important regions of interest in RS applications, those pixels with higher magnitude values (derived from PAN image) than an arbitrary threshold (equal to 700) are plotted on some parts of the MS images in Figure 11. These points are displayed in red colour.

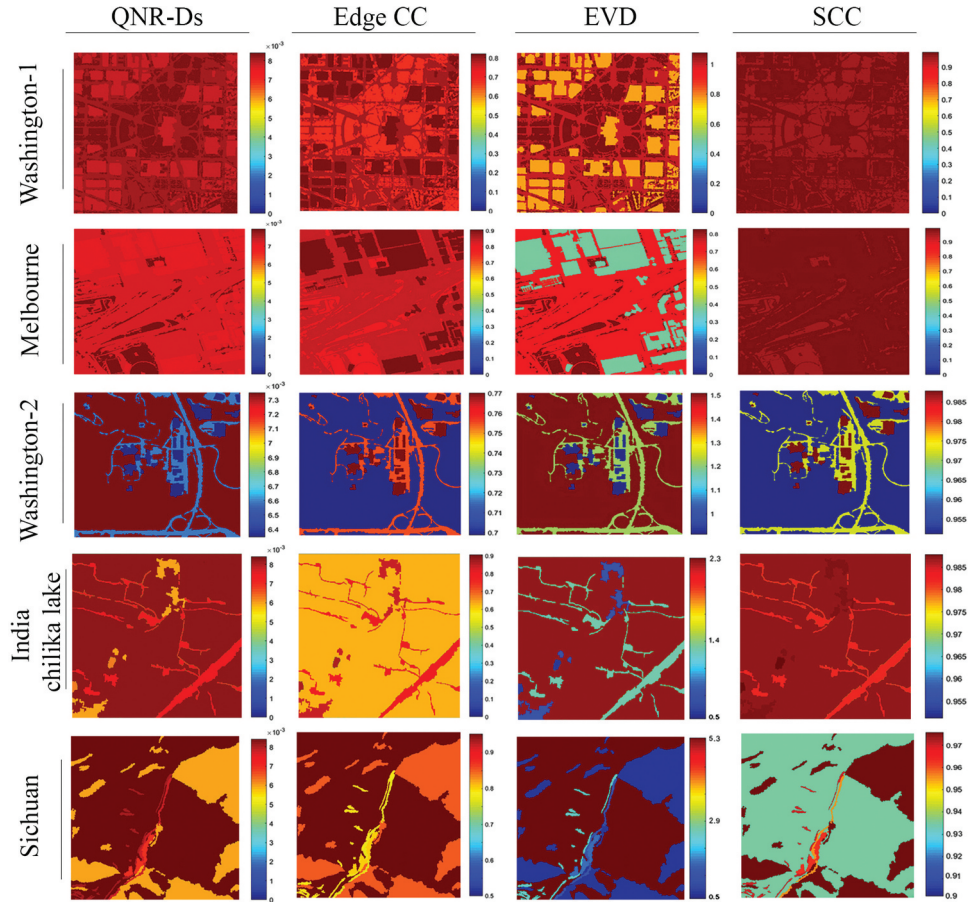


Figure 7. Object-level quality maps of the pan-sharpened images.

The goal is to show how high gradient magnitudes can emphasise the spatially important structures in SQAs.

Regarding the buildings and spatial details detected by the selected gradient threshold in [Figure 11](#), it can be said that the proposed procedure of this paper can even outperform the object-level assessment strategy. This is because the non-sharp pixels inside a building are not supposed to be considered as spatially important pixels in the SQA assessments, while, in object-level evaluations, the whole bunch of pixels belonging to buildings are illogically considered as spatial details.

The ultimate implementations are the quality evaluations accomplished by the proposed weighted SQA method. For this purpose, the SCC, Edge CC, GMS and QNR-Ds are selected to be used as the quality measure. [Table 5](#) is provided to find out how the results of the proposed method differ from conventional pixel-level assessment. The fusion quality results from the proposed and conventional methods are presented in [Table 5](#). For many cases, a considerable difference exists between the results of the proposed and conventional assessments. This is because the space-variant qualities of the pan-sharpened images take part in the final quality score with equal weights when using

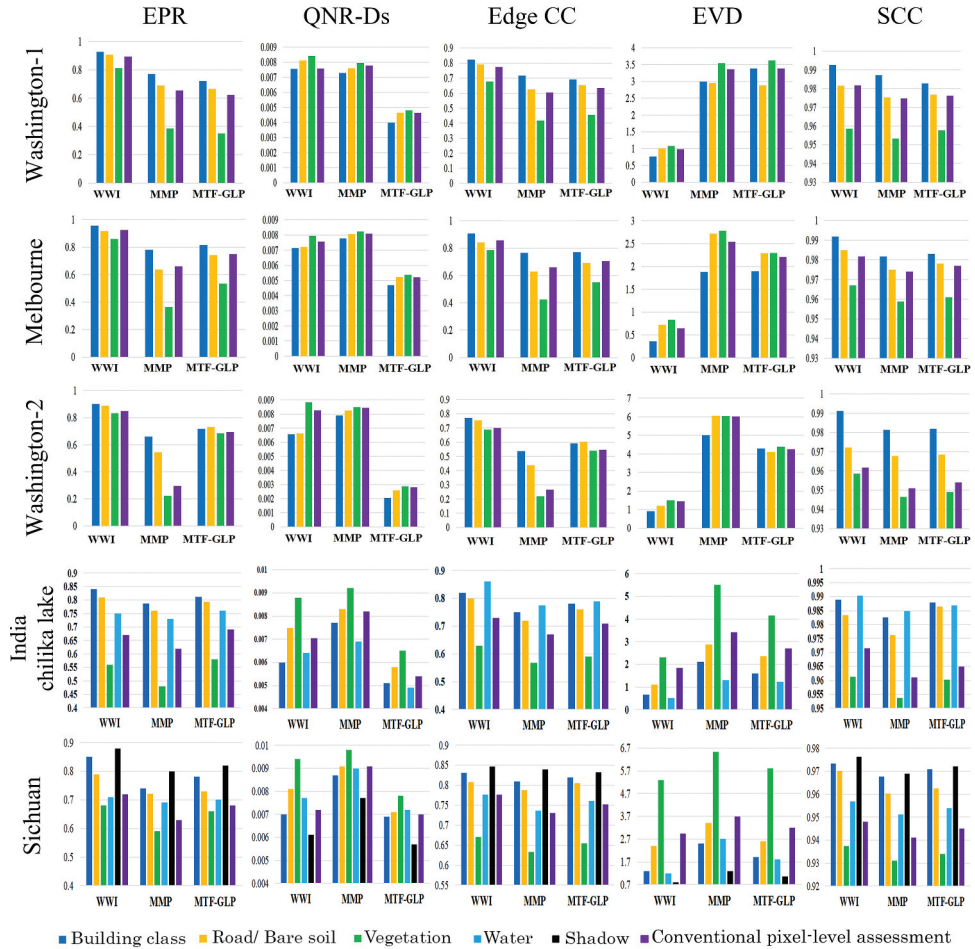


Figure 8. Results of the conventional pixel-level and object-level spatial quality assessment.

conventional assessment. Conversely, the local quality estimations computed in the proposed method participate in the final quality score with different weights that are proportional to the level of the spatial information content in those local regions.

4. Discussion

Conventional pixel-level strategy only renders a unique spatial quality score for the whole pan-sharpened image without considering the image content. In other words, it inherently assigns an identical weight to all image pixels. Based on the results in **Figure 8** and **Table 5**, by the presence of a high percentage of a unique land cover in an image, the conventional pixel-level assessment causes the overall quality score of the image fusion to be so close to the quality result of that extensive land cover. The impact of land covers is great enough to noticeably alter the overall spatial quality of the pan-sharpened images. In particular, the vegetation class of a fused image

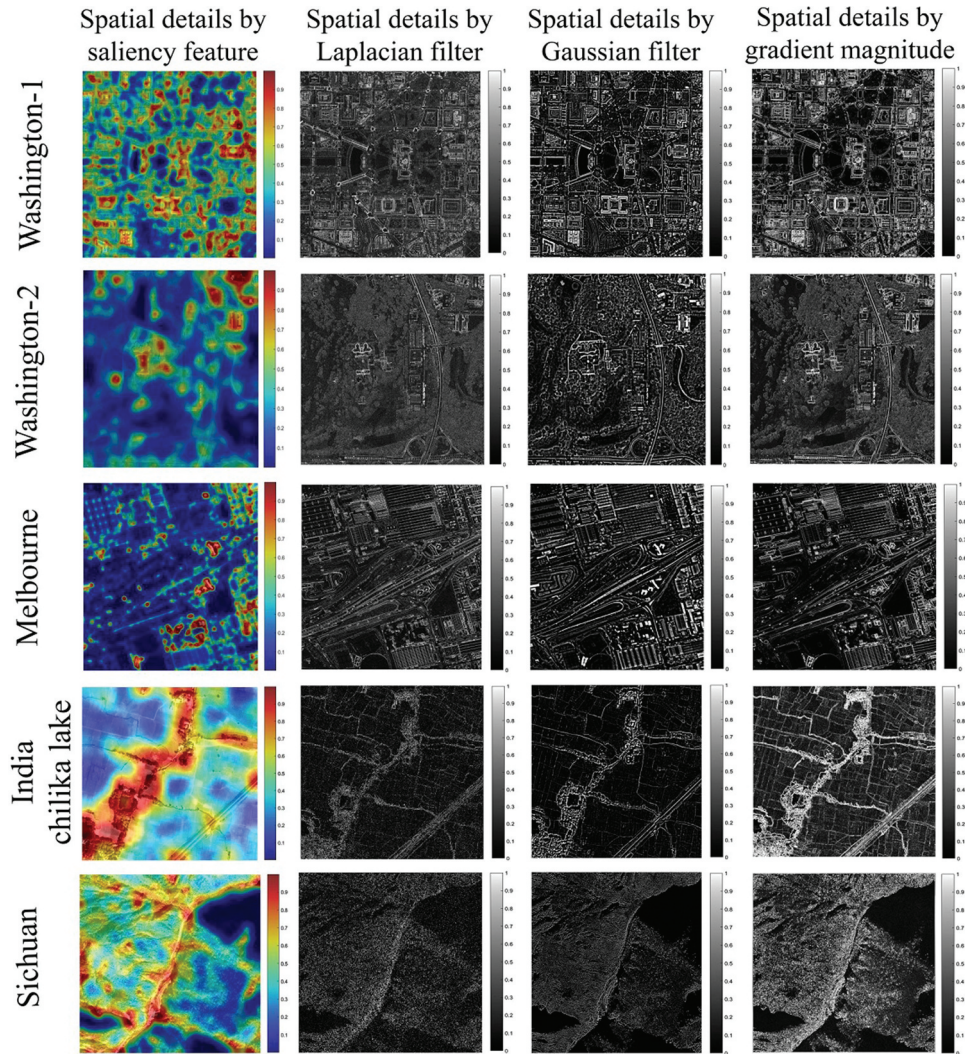


Figure 9. The detail maps extracted from the PAN images, using four spatial feature extraction techniques.

illustrates a significant spatial quality degradation after the fusion, as it is shown in the results of [Figures 5](#), [Figures 6](#), [Figures 7](#) and [Figures 8](#). The shadow class of the IKONOS dataset illustrated high spatial quality preservation. This is probably because there was not much information in shadow to be lost after the fusion. According to the quality maps of [Figures 9](#) and [Figures 10](#), the amount of missed spatial information in the vegetation areas and agricultural regions of a fused image is multiple times more than that of a detailed area. Also, it is shown in [Figure 5](#) that the amount of added (unwanted) edges that did not exist in the PAN image is much more in this class. The reason for large spatial distortions in such areas can be found in the nature of the pan-sharpening function, where almost all pan-sharpening algorithms either provide better spatial quality or a finer spectral performance. The object-level SQA of

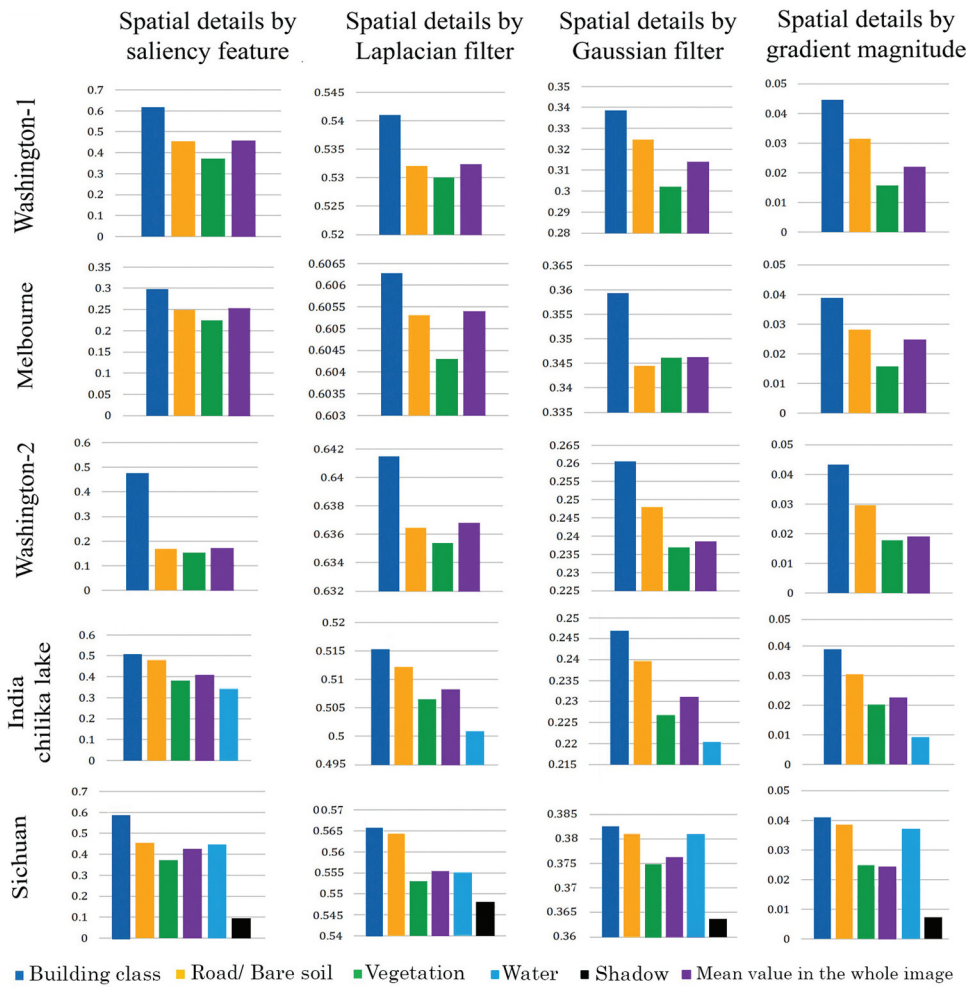


Figure 10. The mean values of the spatial features in separate classes.

this paper indicated that wherever the spectral content of MS data is high, the spatial details of that area cannot be injected into the fused image acceptably, and vice versa. Our illustrated results (Figure 5) show that there are also some extra spatial details in the fused image that are presumably created because of the colour insertion and the contrast they produce after the fusion. In fact, this impact refers to the existence of a slight amount of spatial details in the MS image.

We also found that any quality comparison of fusion methods should be implemented on identical data sets. The issue of comparing the quality of fusion methods that are implemented on different data sets is challenging because of the impact of different image landscapes. Therefore, similar to what is done by Meng *et al.* (2019), any statistical analysis on the quality results of fusion methods which are gathered from various papers without considering the diversity of image contents incorporates an unwanted diversion into the conclusions.

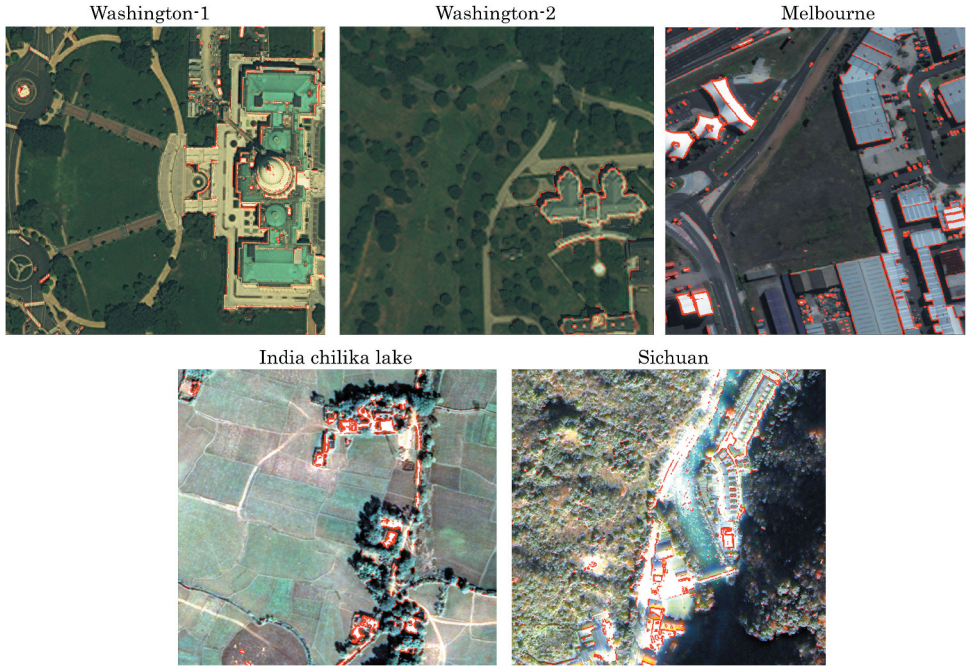


Figure 11. The pixels with magnitude values greater than a threshold of 700 (derived from the PAN image), shown on the MS image and shown in red.

The discussed effect of the type of landscape can be the main answer addressing the question of why the quality result of a specific pan-sharpening method ranges from a fine performance in a satellite image to a weak and low performance in another image. Supposing a specific group of pan-sharpening methods implemented on different satellite images, it is highly likely that anomalous ranking results appear and hence, determining the superior pan-sharpening methods becomes difficult. Based on conventional IQA metrics, one pan-sharpening method can provide a variety of quality ranges if it is implemented for different data images with different landscapes. Since our proposed SQA procedure highly emphasises the spatial structures of images, it is less influenced by non-sharp image regions, hence regardless of the diverse land covers and landscapes, the spatial quality validations of pan-sharpening methods would be more reliably computable. Table 5 depicted that the type of landscape can lead to producing two different spatial quality scores for two cropped images of a single and large satellite image (Washington-1 and Washington-2 datasets). This effect is indispensable, and lower spatial fusion quality in vegetated areas is expectable in comparison with detailed structures. In fact, a dataset highly covered with vegetation is most likely to show poor spatial quality results after the fusion, while the fusion product of a dataset covered with dense buildings, roads and detailed structures presumably attains higher spatial quality. This is the impact of the type of landscape on the fusion quality that we showed in Figures 5, Figures 6, Figures 7 and Figures 8.

The reason why only QNR-Ds has larger values for conventional assessment lies in its reverse ideal value. In QNR-Ds, the ideal value for an image without any distortion is zero. Taking this point into account, the results of QNR-Ds in all datasets are almost consistent with the results of other metrics. In datasets 2 and 3, the difference between the results of the proposed and conventional methods is larger due to the impact of the type of land cover on fusion quality. Datasets 2 and 3 contain less detailed structures, but more vegetation and bare lands. We showed that different land covers show various fusion qualities. Based on our findings in subsection 3.1, the conventional method's result is close to the fusion quality of the most extensive land cover. On the other hand, the proposed method allocates larger weight factors to the quality estimations of detailed areas (i.e. buildings). Contrary to the conventional procedure, the proposed method produces the overall quality score in a way that is close to the fusion quality of detailed areas.

The proposed strategy in this paper can help SQAs from two prospects. First, the impact of the type of landscape on the SQA is being considered. Second, as opposed to conventional methods, the pixels with a high degree of spatial information are taken into account with higher weight factors. According to Figures 10 and Figures 11, almost all important edges of PAN image have had a greater level of gradient magnitude in comparison with flat areas and vegetation covers. The proposed weighted SQA will make these spatial details participate in the SQA with a weight factor that is so much greater than that of flat areas.

Numerous studies in the literature investigated and compared the performance of fusion methods. However, many contradictory results can be found when ranking fusion methods performances. In fact, many well-performed algorithms in a study expose poor performance in other studies and vice versa. The reason probably lies in the lack of an accurate SQA metric. Pan-sharpened images are the inputs of many RS applications (i.e. large-scale mapping of urban areas). The performance of these applications depends on the quality of the pan-sharpened images. Therefore, pan-sharpened images as the inputs of many applications need to be assessed before being used. The proposed framework can reliably reveal the spatial quality of fusion products before any further use.

The IQA methods should not be expert-dependent and time-consuming. Any subjective assessment can easily be affected by many factors, such as the expert's knowledge/interest and image light exposure conditions. In the proposed SQA procedure, we employed a spatial feature for weighting the local qualities instead of land cover information. Therefore, we proposed an automatic SQA method by which different users achieve the same result for the same pan-sharpened image. The proposed procedure does not need any interference from the analyst.

5. Conclusions

A conventional SQA of pan-sharpened images provides a quality score for a complete image assuming an equal fusion quality for all image regions. By assessing the functionality of fusion methods in response to different land covers, this study showed that the spatial quality of man-made structures is higher than that of vegetation areas, regardless of the type of fusion method. Object-level SQA provides local quality estimations in contrast to traditional pixel-level SQA that allocates identical spatial quality to all image pixels. However, object-level SQA is also problematic, as for instance, homogeneous areas inside the roofs of

buildings do not have the same spatial quality as the borders. Traditional pixel-level SQA of pan-sharpened images assigns identical importance to all image pixels participating in spatial SQA. To overcome these shortcomings, we proposed a spatially varying weighted procedure for SQA. It considers locally different qualities and allocates unique weights to every single pixel proportional to its level of spatial information content. It presents a scheme for incorporating the proposed weighted procedure into most conventional spatial metrics. The proposed SQA procedure is recommended for any application of pan-sharpened images, especially those that highly rely upon the spatial quality of the fused images. Future research would be needed to examine the application of the other operators, such as the Canny operator, instead of the Sobel operator in the edge-based SQA metrics. As an open-ended topic, we note that pan-sharpening algorithms and evaluations deserve more content-aware investigations to provide additional purpose-oriented outcomes. Besides, prioritising and regularising fusion in terms of spatial or spectral qualities for different land covers in intended applications can be a practical challenge in the future.

Disclosure statement

No potential conflict of interest was reported by the author(s).

Funding

This research did not receive any specific grant from funding agencies in the public, commercial, or not-for-profit sectors.

ORCID

Farzaneh Dadrass Javan  <http://orcid.org/0000-0002-0910-8160>
 Farhad Samadzadegan  <http://orcid.org/0000-0003-3439-5648>

References

- Agudelo-Medina, O.A., et al., 2019. Perceptual quality assessment of pan-sharpened images. *Remote Sensing*, 11 (7), 877. Multidisciplinary Digital Publishing Institute. doi:[10.3390/rs11070877](https://doi.org/10.3390/rs11070877)
- Aiazzi, B., et al., 2006. MTF-tailored multiscale fusion of high-resolution MS and pan imagery. *Photogrammetric Engineering & Remote Sensing*, 72 (5), 591–596. American Society for Photogrammetry and Remote Sensing. doi:[10.14358/PERS.72.5.591](https://doi.org/10.14358/PERS.72.5.591)
- Aiazzi, B., et al., 2002. Context-driven fusion of high spatial and spectral resolution images based on oversampled multiresolution analysis. *IEEE Transactions on Geoscience and Remote Sensing*, 40 (10), 2300–2312. IEEE. doi:[10.1109/TGRS.2002.803623](https://doi.org/10.1109/TGRS.2002.803623)
- Aiazzi, B., et al. 2012. Twenty-five years of pansharpening: a critical review and new developments. In *Signal and Image Processing for Remote Sensing*, 552–599. Boca Raton, FL, USA:CRC Press.
- Alimuddin, I., Sumantyo, J.T.S., and Kuze, H., 2012. Assessment of pan-sharpening methods applied to image fusion of remotely sensed multi-band data. *International Journal of Applied Earth Observation and Geoinformation*, 18, 165–175. Elsevier. doi:[10.1016/j.jag.2012.01.013](https://doi.org/10.1016/j.jag.2012.01.013)

- Alparone, L., et al., 2008. Multispectral and panchromatic data fusion assessment without reference. *Photogrammetric Engineering & Remote Sensing*, 74 (2), 193–200. American Society for Photogrammetry and Remote Sensing. doi:[10.14358/PERS.74.2.193](https://doi.org/10.14358/PERS.74.2.193)
- Alparone, L., Garzelli, A., and Vivone, G. 2018. Spatial consistency for full-scale assessment of pansharpening. In *IGARSS 2018-2018 IEEE International Geoscience and Remote Sensing Symposium*, 5132–5134. IEEE, Valencia, Spain.
- Alparone, L., et al., 2007. Comparison of pansharpening algorithms: outcome of the 2006 GRS-S data-fusion contest. *IEEE Transactions on Geoscience and Remote Sensing*, 45 (10), 3012–3021. IEEE. doi:[10.1109/TGRS.2007.904923](https://doi.org/10.1109/TGRS.2007.904923)
- Al-Wassai, F.A. and Kalyankar, D.N.V., 2012. *A novel metric approach evaluation for the spatial enhancement of pan-sharpened images*. ArXiv Preprint ArXiv, 1207.5064, Chennai, India.
- Benz, U.C., et al., 2004. Multi-resolution, object-oriented fuzzy analysis of remote sensing data for GIS-ready information. *ISPRS Journal of Photogrammetry and Remote Sensing*, 58 (3–4), 239–258. Elsevier. doi:[10.1016/j.isprsjprs.2003.10.002](https://doi.org/10.1016/j.isprsjprs.2003.10.002)
- Bovolo, F., et al., 2009. Analysis of the effects of pansharpening in change detection on VHR images. *IEEE Geoscience and Remote Sensing Letters*, 7 (1), 53–57. IEEE. doi:[10.1109/LGRS.2009.2029248](https://doi.org/10.1109/LGRS.2009.2029248)
- Castillejo-González, I.L., 2018. Mapping of olive trees using pansharpened quickbird images: an evaluation of pixel-and object-based analyses. *Agronomy*, 8 (12), 288. Multidisciplinary Digital Publishing Institute. doi:[10.3390/agronomy8120288](https://doi.org/10.3390/agronomy8120288)
- Chirici, G., et al., 2016. A meta-analysis and review of the literature on the k-nearest neighbors technique for forestry applications that use remotely sensed data. *Remote Sensing of Environment*, 176, 282–294. Elsevier. doi:[10.1016/j.rse.2016.02.001](https://doi.org/10.1016/j.rse.2016.02.001)
- Choi, M., et al., 2005. Fusion of multispectral and panchromatic satellite images using the curvelet transform. *IEEE Geoscience and Remote Sensing Letters*, 2 (2), 136–140. IEEE. doi:[10.1109/LGRS.2005.845313](https://doi.org/10.1109/LGRS.2005.845313)
- DadrasJavan, F. and Samadzadegan, F., 2014. An object-level strategy for pan-sharpening quality assessment of high-resolution satellite imagery. *Advances in Space Research*, 54 (11), 2286–2295. Elsevier. doi:[10.1016/j.asr.2014.08.024](https://doi.org/10.1016/j.asr.2014.08.024)
- DadrasJavan, F., Samadzadegan, F., and Fathollahi, F., 2018. Spectral and spatial quality assessment of IHS and wavelet based pan-sharpening techniques for high resolution satellite imagery. *Advances in Image and Video Processing*, 6 (2), 1.
- Darwish, A., Leukert, K., and Reinhardt, W. 2003. Image segmentation for the purpose of object-based classification. In *International Geoscience and Remote Sensing Symposium*, 3: III-2039, Toulouse, France.
- Dehnavi, S. and Mohammadzadeh, A., 2015. New edge adaptive GIHS-BT-SFIM fusion method and class-based approach investigation. *International Journal of Image and Data Fusion*, 6 (1), 65–78. Taylor & Francis. doi:[10.1080/19479832.2014.959566](https://doi.org/10.1080/19479832.2014.959566)
- Du, Q., et al., 2007. On the performance evaluation of pan-sharpening techniques. *IEEE Geoscience and Remote Sensing Letters*, 4 (4), 518–522. IEEE. doi:[10.1109/LGRS.2007.896328](https://doi.org/10.1109/LGRS.2007.896328)
- Duran, J., et al., 2017. A survey of pansharpening methods with a new band-decoupled variational model. *ISPRS Journal of Photogrammetry and Remote Sensing*, 125, 78–105. Elsevier. doi:[10.1016/j.isprsjprs.2016.12.013](https://doi.org/10.1016/j.isprsjprs.2016.12.013)
- Ehlers, M., et al., 2010. Multi-sensor image fusion for pansharpening in remote sensing. *International Journal of Image and Data Fusion*, 1 (1), 25–45. Taylor & Francis. doi:[10.1080/19479830903561985](https://doi.org/10.1080/19479830903561985)
- Ferzli, R. and Karam, L.J., 2009. A no-reference objective image sharpness metric based on the notion of Just Noticeable Blur (JNB). *IEEE Transactions on Image Processing*, 18 (4), 717–728. IEEE. doi:[10.1109/TIP.2008.2011760](https://doi.org/10.1109/TIP.2008.2011760)
- Freire, S., et al., 2014. Introducing mapping standards in the quality assessment of buildings extracted from very high resolution satellite imagery. *ISPRS Journal of Photogrammetry and Remote Sensing*, 90, 1–9. Elsevier. doi:[10.1016/j.isprsjprs.2013.12.009](https://doi.org/10.1016/j.isprsjprs.2013.12.009)

- Gilbertson, J.K., Kemp, J., and Adriaan Van, N., 2017. Effect of pan-sharpening multi-temporal Landsat 8 imagery for crop type differentiation using different classification techniques. *Computers and Electronics in Agriculture*, 134, 151–159. Elsevier. doi:[10.1016/j.compag.2016.12.006](https://doi.org/10.1016/j.compag.2016.12.006)
- Guo, C., Qi, Ma., and Zhang, L. 2008. Spatio-temporal saliency detection using phase spectrum of quaternion Fourier transform. In *2008 IEEE Conference on Computer Vision and Pattern Recognition*, 1–8. IEEE, Anchorage, AK, USA.
- Hasanlou, M. and Saradjian, M.R., 2016. Quality assessment of pan-sharpening methods in high-resolution satellite images using radiometric and geometric index. *Arabian Journal of Geosciences*, 9 (1), 45. Springer. doi:[10.1007/s12517-015-2015-0](https://doi.org/10.1007/s12517-015-2015-0)
- Hlatshwayo, S.T., et al., 2019. Mapping forest aboveground biomass in the reforested Buffelsdraai landfill site using texture combinations computed from SPOT-6 pan-sharpened imagery. *International Journal of Applied Earth Observation and Geoinformation*, 74, 65–77. Elsevier. doi:[10.1016/j.jag.2018.09.005](https://doi.org/10.1016/j.jag.2018.09.005)
- Hong, Y., Ren, G., and Liu, E., 2016. A no-reference image blurriness metric in the spatial domain. *Optik*, 127 (14), 5568–5575. Elsevier. doi:[10.1016/j.ijleo.2016.03.077](https://doi.org/10.1016/j.ijleo.2016.03.077)
- Hou, X. and Zhang, L. 2007. Saliency detection: a spectral residual approach. In *2007 IEEE Conference on Computer Vision and Pattern Recognition*, 1–8. IEEE, Minneapolis, MN, USA.
- Ilk, H.G., Jane, O., and Ilk, Ö., 2011. The effect of Laplacian filter in adaptive unsharp masking for infrared image enhancement. *Infrared Physics & Technology*, 54 (5), 427–438. Elsevier. doi:[10.1016/j.infrared.2011.06.002](https://doi.org/10.1016/j.infrared.2011.06.002)
- Jagalingam, P. and Hegde, A.V., 2015. A review of quality metrics for fused image. *Aquatic Procedia*, 4 (Icwrcoe), 133–142. Elsevier. doi:[10.1016/j.aqpro.2015.02.019](https://doi.org/10.1016/j.aqpro.2015.02.019)
- Javan, F.D., Samadzadegan, F., and Reinartz, P., 2013. Spatial quality assessment of pan-sharpened high resolution satellite imagery based on an automatically estimated edge based metric. *Remote Sensing*, 5 (12), 6539–6559. Multidisciplinary Digital Publishing Institute. doi:[10.3390/rs5126539](https://doi.org/10.3390/rs5126539)
- Javan, F.D., et al., 2021. A review of image fusion techniques for pan-sharpening of high-resolution satellite imagery. *ISPRS Journal of Photogrammetry and Remote Sensing*, 171, 101–117. Elsevier. doi:[10.1016/j.isprsjprs.2020.11.001](https://doi.org/10.1016/j.isprsjprs.2020.11.001)
- Javan, F.D., et al., 2019. A review on spatial quality assessment methods for evaluation of pan-sharpened satellite imagery. *The International Archives of Photogrammetry, Remote Sensing and Spatial Information Sciences*, 42, 255–261. Copernicus GmbH. doi:[10.5194/isprs-archives-XLII-4-W18-255-2019](https://doi.org/10.5194/isprs-archives-XLII-4-W18-255-2019)
- Trimble Documentation, 2014. *Eognition developer reference book 9.0*. Germany: Trimble Documentation München.
- Jing, L. and Cheng, Q., 2009. Two improvement schemes of PAN modulation fusion methods for spectral distortion minimization. *International Journal of Remote Sensing*, 30 (8), 2119–2131. Taylor & Francis. doi:[10.1080/01431160802549260](https://doi.org/10.1080/01431160802549260)
- Jing, L. and Cheng, Q., 2011a. An image fusion method for misaligned panchromatic and multi-spectral data. *International Journal of Remote Sensing*, 32 (4), 1125–1137. Taylor & Francis. doi:[10.1080/01431160903527405](https://doi.org/10.1080/01431160903527405)
- Jing, L. and Cheng, Q., 2011b. An image fusion method taking into account phenological analogies and haze. *International Journal of Remote Sensing*, 32 (6), 1675–1694. Taylor & Francis. doi:[10.1080/01431161003621593](https://doi.org/10.1080/01431161003621593)
- Kang, X., Shutao, L., and Benediktsson, J.A., 2013. Pan sharpening with matting model. *IEEE Transactions on Geoscience and Remote Sensing*, 52 (8), 5088–5099. IEEE. doi:[10.1109/TGRS.2013.2286827](https://doi.org/10.1109/TGRS.2013.2286827)
- Karam, L.J., et al., 2009. Introduction to the issue on visual media quality assessment. *IEEE Journal of Selected Topics in Signal Processing*, 3 (2), 189–192. IEEE. doi:[10.1109/JSTSP.2009.2015485](https://doi.org/10.1109/JSTSP.2009.2015485)
- Khan, M.M., Alparone, L., and Chanussot, J., 2009. Pansharpening quality assessment using the modulation transfer functions of instruments. *IEEE Transactions on Geoscience and Remote Sensing*, 47 (11), 3880–3891. IEEE. doi:[10.1109/TGRS.2009.2029094](https://doi.org/10.1109/TGRS.2009.2029094)

- Klonus, S. and Ehlers, M. **2009**. Performance of evaluation methods in image fusion. In *2009 12th International Conference on Information Fusion*, 1409–1416. IEEE, Seattle, WA, USA.
- Li, H., Jing, L., and Tang, Y., **2017**. Assessment of pansharpening methods applied to worldview-2 imagery fusion. *Sensors*, 17 (1), 89. Multidisciplinary Digital Publishing Institute. doi:[10.3390/s17010089](https://doi.org/10.3390/s17010089)
- Li, H. and Jing, L., **2017**. Improvement of a pansharpening method taking into account haze. *IEEE Journal of Selected Topics in Applied Earth Observations and Remote Sensing*, 10 (11), 5039–5055. IEEE. doi:[10.1109/JSTARS.2017.2730221](https://doi.org/10.1109/JSTARS.2017.2730221)
- Li, H., et al., **2018**. An improved pansharpening method for misaligned panchromatic and multi-spectral data. *Sensors*, 18 (2), 557. Multidisciplinary Digital Publishing Institute. doi:[10.3390/s18020557](https://doi.org/10.3390/s18020557)
- Liu, Q., Huang, C., and He, L., **2020**. Quality assessment by region and land cover of sharpening approaches applied to GF-2 imagery. *Applied Sciences*, 10 (11), 3673. Multidisciplinary Digital Publishing Institute. doi:[10.3390/app10113673](https://doi.org/10.3390/app10113673)
- Makarau, A., Palubinskas, G., and Reinartz, P., **2012**. Analysis and selection of pan-sharpening assessment measures. *Journal of Applied Remote Sensing*, 6 (1), 63548. International Society for Optics and Photonics. doi:[10.1117/1.JRS.6.063548](https://doi.org/10.1117/1.JRS.6.063548)
- Meng, X., et al., **2018**. Pansharpening for cloud-contaminated very high-resolution remote sensing images. *IEEE Transactions on Geoscience and Remote Sensing*, 57 (5), 2840–2854. IEEE. doi:[10.1109/TGRS.2018.2878007](https://doi.org/10.1109/TGRS.2018.2878007)
- Meng, X., et al. **2019**. Review of the pansharpening methods for remote sensing images based on the idea of meta-analysis: practical discussion and challenges. *Information Fusion*, 46, 102–113. Elsevier B.V. doi:[10.1016/j.inffus.2018.05.006](https://doi.org/10.1016/j.inffus.2018.05.006)
- Mitchell, H.B., **2010**. *Image fusion: theories, techniques and applications*. Springer Science & Business Media, Springer-Verlag Berlin Heidelberg.
- Moghim, A., et al., **2020**. A novel radiometric control set sample selection strategy for relative radiometric normalization of multitemporal satellite images. *IEEE Transactions on Geoscience and Remote Sensing*, 59 (3), 2503–2519. IEEE. doi:[10.1109/TGRS.2020.2995394](https://doi.org/10.1109/TGRS.2020.2995394)
- Mohammadzadeh, A., Tavakoli, A., and Valadan Zanj, M.J., **2006**. Road extraction based on fuzzy logic and mathematical morphology from pan-sharpened Ikonos images. *The Photogrammetric Record*, 21 (113), 44–60. Wiley Online Library. doi:[10.1111/j.1477-9730.2006.00353.x](https://doi.org/10.1111/j.1477-9730.2006.00353.x)
- Nichol, J. and Wong, M.S., **2005**. Satellite remote sensing for detailed landslide inventories using change detection and image fusion. *International Journal of Remote Sensing*, 26 (9), 1913–1926. Taylor & Francis. doi:[10.1080/01431160512331314047](https://doi.org/10.1080/01431160512331314047)
- Nikolakopoulos, K. and Oikonomidis, D., **2015**. Quality assessment of ten fusion techniques applied on worldview-2. *European Journal of Remote Sensing*, 48 (1), 141–167. Taylor & Francis. doi:[10.5721/EuJRS20154809](https://doi.org/10.5721/EuJRS20154809)
- Ni, Z., et al. **2016**. Screen content image quality assessment using edge model. In *2016 IEEE International Conference on Image Processing (ICIP)*, 81–85. IEEE, Phoenix, AZ, USA.
- Palubinskas, G., **2015**. Joint quality measure for evaluation of pansharpening accuracy. *Remote Sensing*, 7 (7), 9292–9310. Multidisciplinary Digital Publishing Institute. doi:[10.3390/rs70709292](https://doi.org/10.3390/rs70709292)
- Pardo-Igúzquiza, E., Chica-Olmo, M., and Atkinson, P.M., **2006**. Downscaling cokriging for image sharpening. *Remote Sensing of Environment*, 102 (1–2), 86–98. Elsevier. doi:[10.1016/j.rse.2006.02.014](https://doi.org/10.1016/j.rse.2006.02.014)
- Pardo-Igúzquiza, E. and Atkinson, P.M., **2007**. Modelling the semivariograms and cross-semivariograms required in downscaling cokriging by numerical convolution–deconvolution. *Computers & Geosciences*, 33 (10), 1273–1284. Elsevier. doi:[10.1016/j.cageo.2007.05.004](https://doi.org/10.1016/j.cageo.2007.05.004)
- Pardo-Igúzquiza, E., Atkinson, P.M., and Chica-Olmo, M., **2010**. DSCOKRI: a library of computer programs for downscaling cokriging in support of remote sensing applications. *Computers & Geosciences*, 36 (7), 881–894. Elsevier. doi:[10.1016/j.cageo.2009.10.006](https://doi.org/10.1016/j.cageo.2009.10.006)
- Pushparaj, J. and Hegde, A.V., **2017**. Evaluation of pan-sharpening methods for spatial and spectral quality. *Applied Geomatics*, 9 (1), 1–12. Springer. doi:[10.1007/s12518-016-0179-2](https://doi.org/10.1007/s12518-016-0179-2)

- Qi, H., et al., 2014. Content-based image quality assessment using semantic information and luminance differences. *Electronics Letters*, 50 (20), 1435–1436. IET. doi:[10.1049/el.2014.1651](https://doi.org/10.1049/el.2014.1651)
- Qin, Y., et al. 2015. Saliency detection via cellular automata. In *Proceedings of the IEEE Conference on Computer Vision and Pattern Recognition*, 110–119, Boston, MA, USA.
- Restaino, R., et al., 2016. Context-adaptive pansharpening based on image segmentation. *IEEE Transactions on Geoscience and Remote Sensing*, 55 (2), 753–766. IEEE. doi:[10.1109/TGRS.2016.2614367](https://doi.org/10.1109/TGRS.2016.2614367)
- Rodríguez-Esparragón, D., et al., 2017. Object-based quality evaluation procedure for fused remote sensing imagery. *Neurocomputing*, 255, 40–51. doi:[10.1016/j.neucom.2016.06.091](https://doi.org/10.1016/j.neucom.2016.06.091)
- Samadzadegan, F. and Farzaneh, D., 2011. Evaluating the sensitivity of image fusion quality metrics to image degradation in satellite imagery. *Journal of the Indian Society of Remote Sensing*, 39 (4), 431–441. Springer. doi:[10.1007/s12524-011-0117-z](https://doi.org/10.1007/s12524-011-0117-z)
- Samadzadegan, F. and Javan, F.D., 2013. Image fusion quality assessment of high resolution satellite imagery based on an object level strategy. *International Journal of Image Processing (IJIP)*, 7 (2), 140.
- Seo, H.J. and Milanfar, P., 2009. Static and space-time visual saliency detection by self-resemblance. *Journal of Vision*, 9 (12), 15. The Association for Research in Vision and Ophthalmology. doi:[10.1167/9.12.15](https://doi.org/10.1167/9.12.15)
- Shi, Z., et al., 2018. Full-reference image quality assessment based on image segmentation with edge feature. *Signal Processing*, 145, 99–105. Elsevier. doi:[10.1016/j.sigpro.2017.11.015](https://doi.org/10.1016/j.sigpro.2017.11.015)
- Sirguey, P., et al., 2008. Improving MODIS spatial resolution for snow mapping using wavelet fusion and ARSIS concept. *IEEE Geoscience and Remote Sensing Letters*, 5 (1), 78–82. IEEE. doi:[10.1109/LGRS.2007.908884](https://doi.org/10.1109/LGRS.2007.908884)
- Snehmani, A.G., et al., 2017. A comparative analysis of pansharpening techniques on QuickBird and WorldView-3 images. *Geocarto International*, 32 (11), 1268–1284. Taylor & Francis. doi:[10.1080/10106049.2016.1206627](https://doi.org/10.1080/10106049.2016.1206627)
- Thanh Noi, P. and Kappas, M., 2018. Comparison of random forest, k-nearest neighbor, and support vector machine classifiers for land cover classification using sentinel-2 imagery. *Sensors*, 18 (1), 18. Multidisciplinary Digital Publishing Institute. doi:[10.3390/s18010018](https://doi.org/10.3390/s18010018)
- Thomas, C. and Wald, L. 2004. Assessment of the quality of fused products. In.
- Toosi, A., et al., 2020. Object-based spectral quality assessment of high-resolution pan-sharpened satellite imageries: new combined fusion strategy to increase the spectral quality. *Arabian Journal of Geosciences*, 13 (13), 1–17. Springer. doi:[10.1007/s12517-020-05523-3](https://doi.org/10.1007/s12517-020-05523-3)
- Vivone, G., et al., 2014. A critical comparison among pansharpening algorithms. *IEEE Transactions on Geoscience and Remote Sensing*, 53 (5), 2565–2586. IEEE. doi:[10.1109/TGRS.2014.2361734](https://doi.org/10.1109/TGRS.2014.2361734)
- Wald, L., Ranchin, T., and Mangolini, M., 1997. Fusion of satellite images of different spatial resolutions: assessing the quality of resulting images. *Photogrammetric Engineering and Remote Sensing*, 63 (6), 691–699.
- Wang, Z. and Shang, X. 2006. Spatial pooling strategies for perceptual image quality assessment. In *2006 International Conference on Image Processing*, 2945–2948. IEEE, Atlanta, GA, USA.
- Wang, Z. and Qiang, L., 2010. Information content weighting for perceptual image quality assessment. *IEEE Transactions on Image Processing*, 20 (5), 1185–1198. IEEE. doi:[10.1109/TIP.2010.2092435](https://doi.org/10.1109/TIP.2010.2092435)
- Wang, Z., et al., 2015. A new image quality assessment algorithm based on SSIM and multiple regressions. *International Journal of Signal Processing, Image Processing and Pattern Recognition*, 8 (11), 221–230. doi:[10.14257/ijssip.2015.8.11.20](https://doi.org/10.14257/ijssip.2015.8.11.20)
- Wang, Z. and Bovik, A.C., 2002. A universal image quality index. *IEEE Signal Processing Letters*, 9 (3), 81–84. IEEE. doi:[10.1109/97.995823](https://doi.org/10.1109/97.995823)
- Wang, Q., et al., 2016. Fusion of sentinel-2 images. *Remote Sensing of Environment*, 187, 241–252. Elsevier. doi:[10.1016/j.rse.2016.10.030](https://doi.org/10.1016/j.rse.2016.10.030)
- Wang, Q., Shi, W., and Atkinson, P.M., 2019. Information loss-guided multi-resolution image fusion. *IEEE Transactions on Geoscience and Remote Sensing*, 58 (1), 45–57. IEEE. doi:[10.1109/TGRS.2019.2930764](https://doi.org/10.1109/TGRS.2019.2930764)

- Wen, Y., et al., 2017. A weighted full-reference image quality assessment based on visual Saliency. *Journal of Visual Communication and Image Representation*, 43, 119–126. Elsevier. doi:[10.1016/j.jvcir.2016.12.005](https://doi.org/10.1016/j.jvcir.2016.12.005)
- Xing, Y., et al., 2018. Pan-sharpening via deep metric learning. *ISPRS Journal of Photogrammetry and Remote Sensing*, 145, 165–183. Elsevier. doi:[10.1016/j.isprsjprs.2018.01.016](https://doi.org/10.1016/j.isprsjprs.2018.01.016)
- Xue, W., et al., 2013. Gradient magnitude similarity deviation: a highly efficient perceptual image quality index. *IEEE Transactions on Image Processing*, 23 (2), 684–695. IEEE. doi:[10.1109/TIP.2013.2293423](https://doi.org/10.1109/TIP.2013.2293423)
- Yu, S., et al. 2014. Applications of edge preservation ratio in image processing. In 2014 12th International Conference on Signal Processing (ICSP), 698–702. IEEE, Hangzhou, China.
- Zhang, X., et al., 2013. Edge strength similarity for image quality assessment. *IEEE Signal Processing Letters*, 20 (4), 319–322. IEEE. doi:[10.1109/LSP.2013.2244081](https://doi.org/10.1109/LSP.2013.2244081)
- Zhang, Y., 2008. Methods for image fusion quality assessment-a review, comparison and analysis. *The International Archives of the Photogrammetry, Remote Sensing and Spatial Information Sciences*, 37 (PART B7), 1101–1109. Citeseer.
- Zhang, Y. and Hong, G., 2005. An IHS and wavelet integrated approach to improve pan-sharpening visual quality of natural colour IKONOS and QuickBird images. *Information Fusion*, 6 (3), 225–234. Elsevier. doi:[10.1016/j.inffus.2004.06.009](https://doi.org/10.1016/j.inffus.2004.06.009)
- Zhou, J., Civco, D.L., and Silander, J.A., 1998. A wavelet transform method to merge landsat TM and SPOT panchromatic data. *International Journal of Remote Sensing*, 19 (4), 743–757. Taylor & Francis. doi:[10.1080/014311698215973](https://doi.org/10.1080/014311698215973)